

Geophysical Assessment of the Upper Dja Series Using Electrical Resistivity Data

Zoo Zame P, Mbida Yem*, Yene Atangana JQ and Ekomané E

Department of Earth Sciences, University of Yaounde I, Cameroon

Abstract

The upper Dja series consists of carbonates and shales deposits that date 580 ± 150 Ma. Petrography and mineral chemistry studies helped to differentiate this series into many sequences including massive limestone layers with calcite (CaO₃) contents of about 30 to 42%. In order to determine the subsurface distribution of these sequences, a geophysical prospection campaign was carried out in which a total of 24 vertical resistivity soundings were recorded over a surface area of 9 km². The processing and interpretation of data using the IX1D and OpendTect modeling tools permitted the distinction of two massive limestone layers in the upper Dja series. The first layer of about 10 to 35 m thick and outcrop in few places is characterized by resistivity ranging between 1110 and 2377 Ωm, while the second layer located beyond 50 m deep is separated by a very conductive clay stone layer with a capped thickness of 15 to 35 m. 3D modeling of the top and base of these formations indicates that, the whole Upper Dja series of about 190 m thick presents folded structure. These results can constitute a useful base of information in regards to a large scale economic study of the Upper Dja limestone series.

Keywords: Geophysical prospection; Upper Dja series; Vertical sounding; Limestone layer

Introduction

In Cameroon, limestone neoproterozoic metamorphism is essentially represented by the marble and travertine deposits of Bidzar and the Upper Dja series respectively (Figure 1). Other schisto-calcareous massifs have been indicated in the paleozoic to mesozoic trenches in Figuil, Moungo, Kompina and Logbadjeck. In the Dja series, the zones with the most important limestone deposit were revealed to be in relation with the sedimentary furrow of the Dja River and the Atog-Adjap outcrops [1-8]. These massifs are partially covered by the forest and the Dja phanerozoic basin.

The works of Gazel and Guiraudie and Van Houtte, presented the first observations as well as the early petrographic studies of these massifs [1,2]. More recent studies were carried out by Ntep et al., with aims to study the composition and their contents in calcium carbonate ores. In addition, these works consisted of deep drill cores, geological surveys, rock sampling, description of outcrops and pale environmental analysis [6].

In this study, the main questions were mostly concerned with the continuity and geometry of defined targets through drilling on a surface area of 9 km², with objective to constitute and put at the disposal of scientists and the industrial sector a database of useful information on the large scale evaluation of the upper Dja series of carbonates and perlite reserves.

Geological Context

The upper Dja carbonates series was dated using ²⁰⁷P/²⁰⁴P and ²⁰⁶P/²⁰⁴P isotopes, and the age obtained is 580 ± 150 Ma [6]. This series is hosted in a flexural basin of about 40 km wide. The research permit of this deposit is located between latitudes N 02°40' to 3° and Longitudes E 13° to 13°30', overlapped between a northern over flooded zone and a swampy southern zone. Up till date, most of the known limestone outcrops are found in the flooded (Figure 1).

Morphologically, in some places the very variable relief presents very steep valleys, whose unevenness can attain 30 m. On a geological point of view, the encountered formations are successively made up of:

- A base complex made up of migmatites, dolerites, diorites, granodiorites, amphibolites, granites and gabbro [9,10].
- The Mbalmayo-bengbis series which is essentially made up of chloritoschists [11].
- The upper Dja series made up of perlitites, calcareous schist and clay stone [5,9].
- Phanerozoic formed by a recent sedimentary assembly, it is represented by conglomerates, siliceous sandstone, overlaid by a locally brecciated cuirassed laterite [12].

As well, control drilled boreholes F1 and F2 realized in the perimeters of the study area reveals that the limestone rich massif formations have variable thicknesses as follow [3,4]:

- At borehole F1, situated close to the SE2 and SE3 electrical soundings (Figure 2), limestone massifs extends from 58 m up to 142 m. Its overburden is made of clays and detritic formations from 14 to 58 m overlaid by laterite of about 9 m thick and recent colluvial material at the top of the borehole.
- At borehole F2 situated close to the SE19 electrical soundings, is made up of a clayey colluvial and lateritic cuirass cover on the first 15 meters, followed by an alternation of a massif and shaly limestone up to 103 m. A layer of pelite of about 16 m thick is found below the limestone alternation.

These data permitted the calibration of resistivity profiles by realizing controlled electrical soundings in line with some boreholes.

***Corresponding author:** Mbida Yem, Department of Earth Sciences, University of Yaounde I, Cameroon, Tel: (237) 698134061; E-mail: yem04@yahoo.com

Received April 17, 2017; Accepted May 09, 2017; Published May 16, 2017

Citation: Zame PZ, Yem M, Atangana JQY, Ekomané E (2017) Geophysical Assessment of the Upper Dja Series Using Electrical Resistivity Data. J Geol Geophys 6: 292. doi: 10.4172/2381-8719.1000292

Copyright: © 2017 Zame PZ, et al. This is an open-access article distributed under the terms of the Creative Commons Attribution License, which permits unrestricted use, distribution, and reproduction in any medium, provided the original author and source are credited.

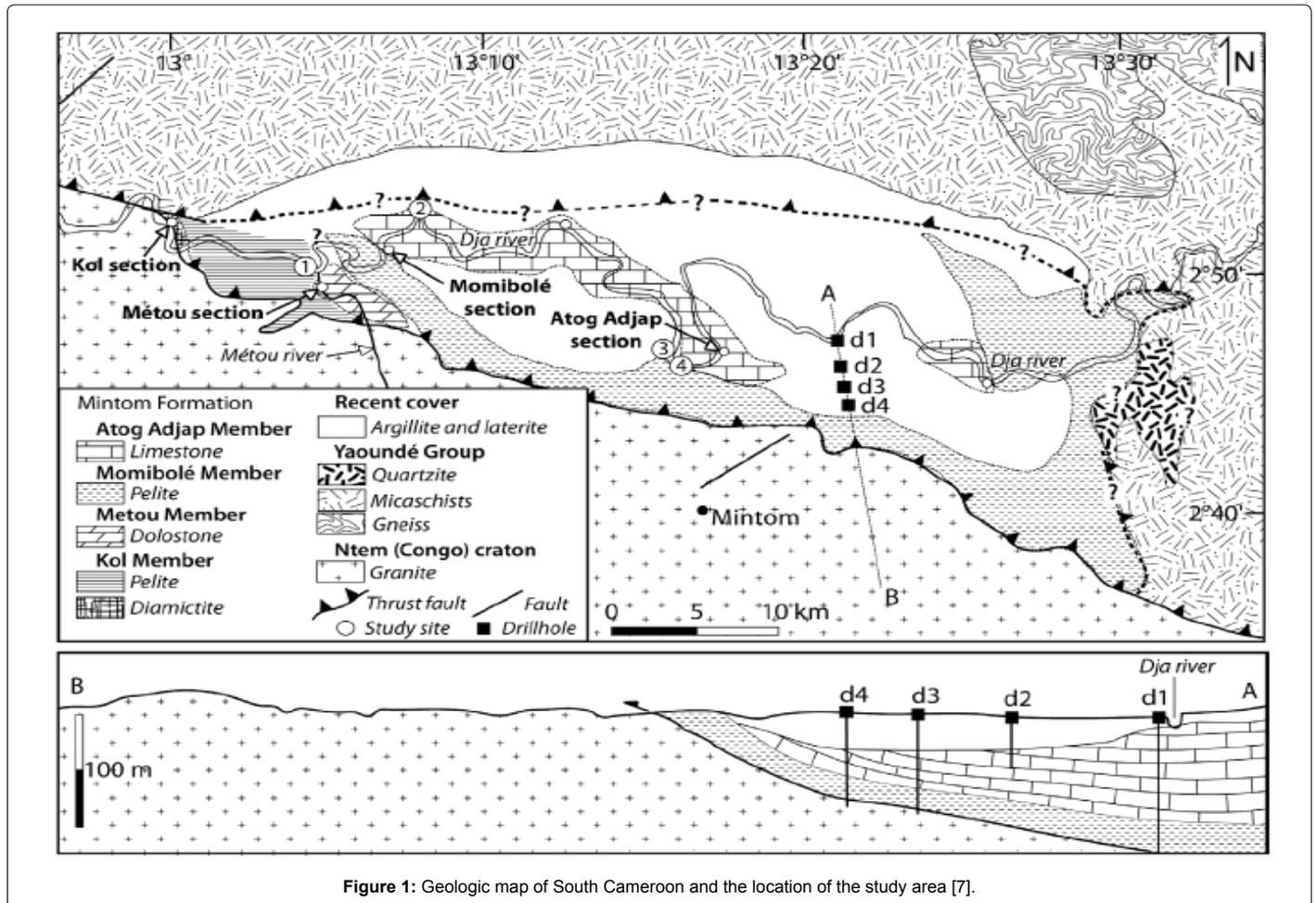


Figure 1: Geologic map of South Cameroon and the location of the study area [7].

Data and Methods

Geophysical methods represent important tools in the spatial characterization of geological formations [13]. Electrical resistivity mapping is an example of such well-developed methods and have been widely applied in the study of geological formations in the humid intertropical zone [14-17]. This method is particularly adapted in the study of subsurface discontinuity, marked by vertical and horizontal juxtaposition of geologic formations with well contrasted electrical properties. In vertical structures of homogenous milieu, where resistivity changes with depth, vertical electrical sounding has been identified to be the most adapted method. In the present study, this method was conducted following 24 profile lines with four over the core drilling boreholes (Figure 2). The Schlumberger electrode configuration with was use for the purpose to attain the maximum depth of the carbonate series as well as the top of the basement rock.

Vertical electrical sounding is a geophysical prospecting method for deep subsurface exploration [13,18,19]. Classically, the minimum size of subsurface anomalies investigated by vertical electrical sounding depends on the type of electrode array used as well as its physical dimension [13]. Theoretically, it has been shown that the Schlumberger configuration permits topographic corrections and it is very sensible to vertical resistivity variations [20,21]. In this study, the Schlumberger configuration was used with current electrode spacing varying from 12 to 500 m.

According to Abraham Bairu, the calculation of apparent resistivity values in the case of Schlumberger configuration is expressed by:

$$\rho_a = K \Delta V / I$$

where: ΔV is the potential difference; I is the current intensity.

K is the geometric factor, which depends on the arrangement of electrodes.

For a AMNB electrode array, $K = \pi [(AB/2)^2 - (MN/2)^2] / MN$, with A-B being the current electrodes; M-N being the potential difference electrodes.

The spatial orientation and position of profile lines collected using this configuration is represented in Table 1. In order to determine geoelectrical sequences (Figure 3) over each sounding points, a software processing was done with the aid of the IX1D/RES2DINV codes [22].

Geoelectrical Correlations and Interpretations

Geoelectrical sequences

With reference to the overall vertical sounding curves, it is seen that, the underground cutting between the topographic surface (altitude ~ 640 m) and the bedrock substratum (altitude ~ 430 m) is made up of five (05) geoelectrical sequences, labeled: e1, e2, e3, e4 and e5 (Table 2).

Geoelectrical sequence e1

This sequence is situated at the top of the sedimentary section

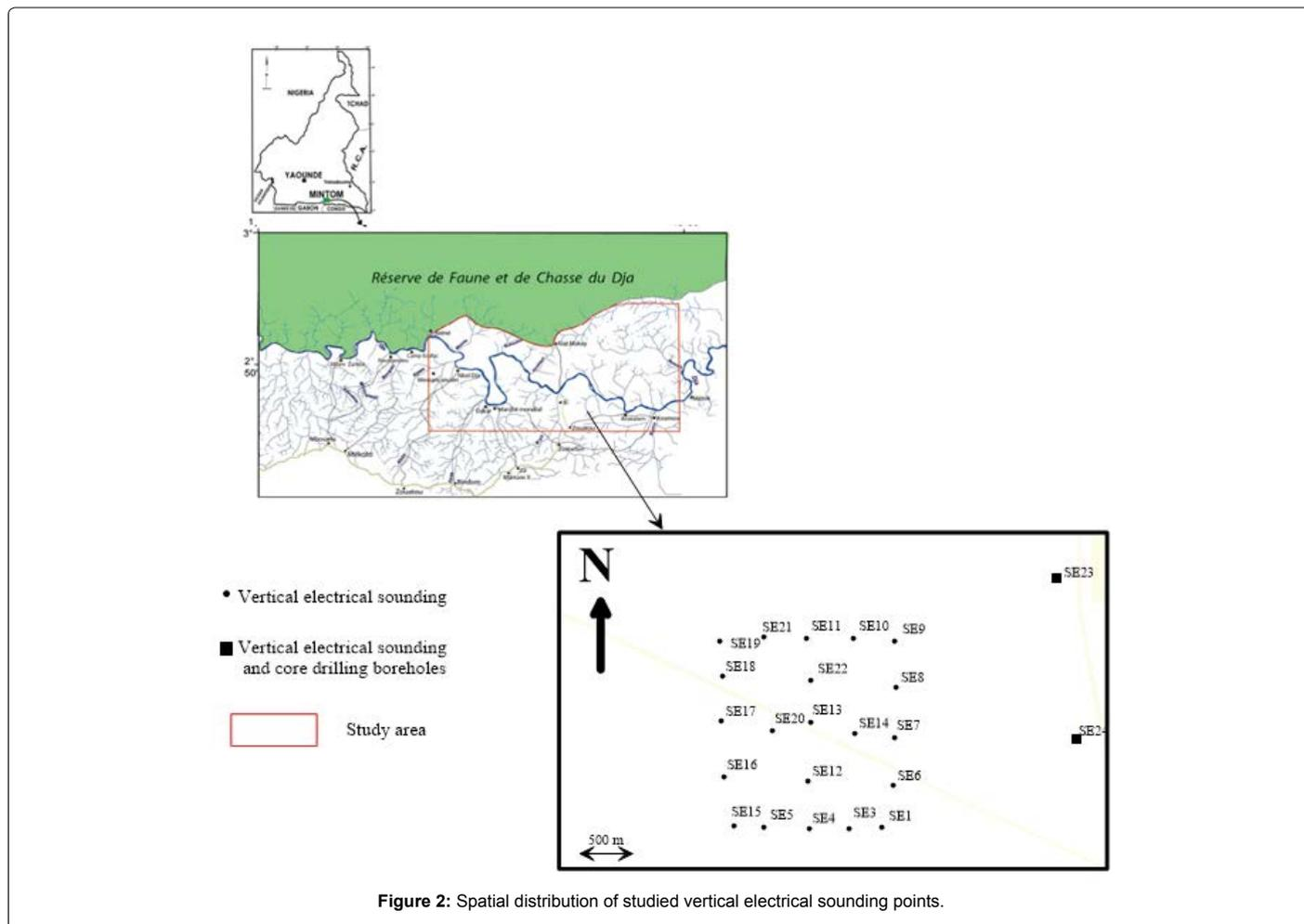


Figure 2: Spatial distribution of studied vertical electrical sounding points.

No.	Azimut	AB/2	X	Y	Z
SE1	E-W	150	E 13° 19' 35,4"	N02° 46' 00,7"	615
SE2	E-W	150	E13° 19' 30,6"	N02° 46' 00,6"	632
SE3	E-W	150	E13° 19' 12,5"	N02° 46' 00,3"	635
SE4	E-W	150	E13° 18' 49,9"	N02° 45' 59,7"	626
SE5	E-W	150	E13° 18' 23,2"	N02° 46' 01,2"	634
SE6	N-S	200	E13° 19' 37,0"	N02° 46' 22,2"	623
SE7	N-S	150	E13° 19' 37,6"	N02° 46' 48,5"	591
SE8	N-S	150	E13° 19' 39,4"	N02° 47' 15,0"	575
SE9	N-S	150	E13° 19' 40,6"	N02° 47' 39,4"	570
SE10	E-W	150	E13° 19' 15,2"	N02° 47' 41,2"	593
SE11	E-W	150	E13° 18' 47,7"	N02° 47' 41,4"	580
SE12	N-S	150	E13° 18' 49,9"	N02° 46' 24,3"	609
SE13	N-S	150	E13° 18' 51,1"	N02° 46' 56,6"	616
SE14	E-W	150	E13° 19' 15,4"	N02° 46' 50,1"	579
SE15	E-W	150	E13° 18' 06,4"	N02° 46' 01,9"	620
SE16	N-S	200	E13° 18' 00,6"	N02° 46' 27,3"	588
SE17	N-S	250	E13° 17' 59,5"	N02° 46' 57,5"	577
SE18	N-S	150	E13° 17' 59,9"	N02° 47' 21,3"	611
SE19	N-S	250	E13° 18' 00,7"	N02° 47' 32,1"	627
SE20	E-w	150	E13° 18' 28,1"	N02° 46' 51,9"	628
SE21	E-W	150	E13° 18' 24,3"	N02° 47' 41,3"	580
SE22	N-S	150	E13° 18' 51,0"	N02° 47' 19,4"	616
SE23 (F1)	E-W	250	E13° 21' 10,2"	N02° 48' 09,7"	609
SE24(F2)	E-W	150	E13° 21' 20,6"	N02° 46' 44,9"	566

Table 1: Characteristics of recording vertical electrical sounding.

and in some places, forms the cover terrain of e2. Details analysis of resistivity profiles (Figure 3) reveals that e1 thickness varied between 1 and 20 m. Its thickest section is observed over the sounding 18 (Figure 4a), while its thinnest portion is observed at the sounding points 11 and 21 (Figure 4b). In an electrical point of view, e1 is made up of two units as follow:

- U1: semi-resistive with a resistivity of 826 to 1068 Ωm.
- U2: very resistive with resistivity of 5011 to 13545 Ωm.

This differentiation clearly appears in the sounding point 6 (Figure 4c).

Geoelectrical sequence e2

Just as e1, e2 is also a continuous sequence and the general analysis of sounding curves show that, the thickness of e2 decreases from the western (Figure 4a) towards the eastern (Figure 4c) part of the study area. The resistivity values (1110-2377 Ωm) equally obtained from the inversion of resistivity data reveal that, the physical nature of the e2 turns to degrade from the South towards the North of the study area (Figure 4).

Geoelectrical sequence e3

In an electrical point of view, e3 is a conductive sequence whose resistivity vary between 181 and 746 Ωm. Some sounding curves obtained by resistivity inversion of the data collected in the North and

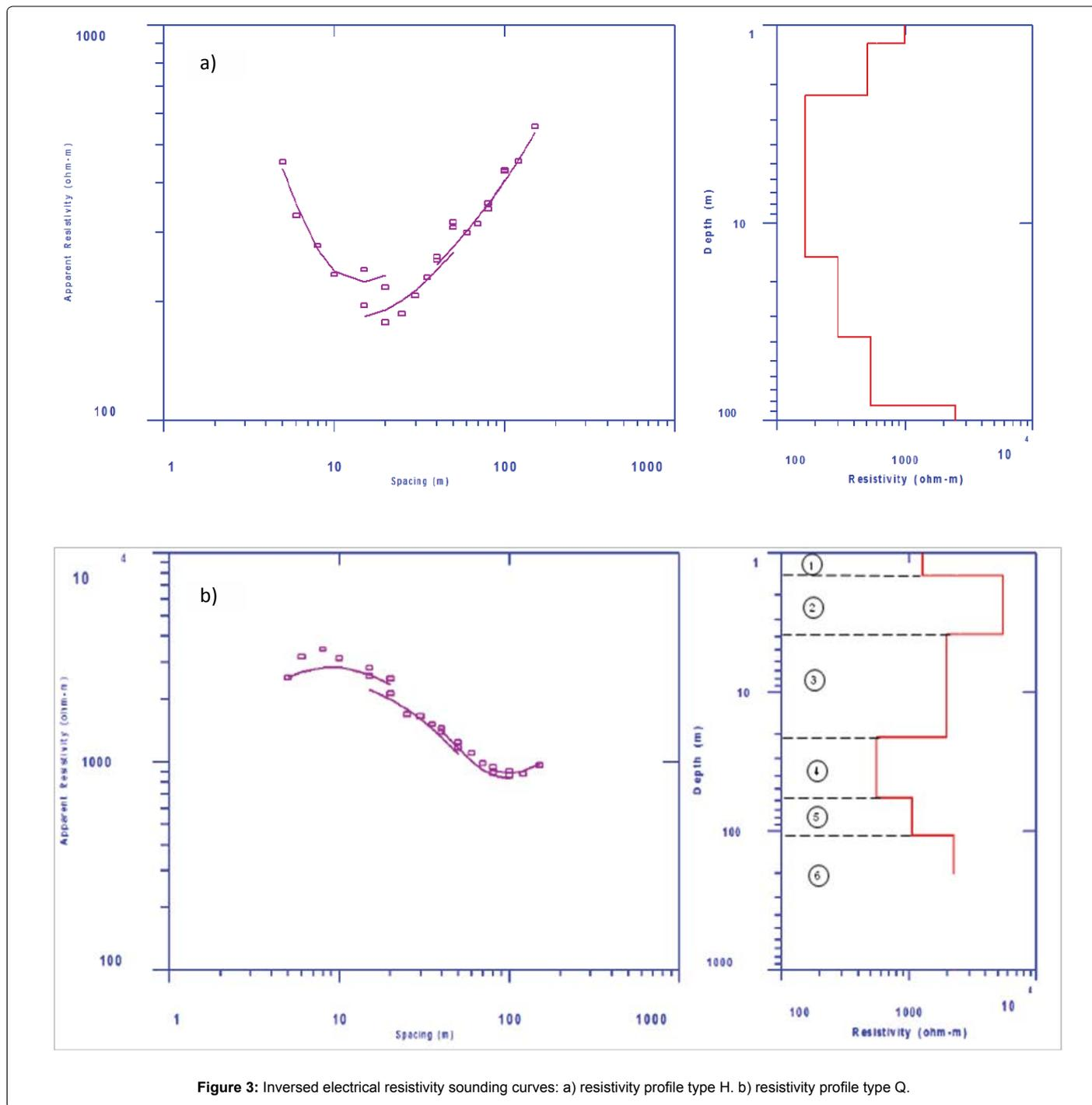


Figure 3: Inversed electrical resistivity sounding curves: a) resistivity profile type H. b) resistivity profile type Q.

Central parts of the study area (Figures 5a and 5b), show that e3 is made up of two units: U4 (conductive) and U5 (semi-conductive, Figure 5b). Contrary to e2, details analysis of the set of electrical pattern indicates that the thickness of e3 increases from the western (Figure 4a) towards the eastern (Figure 4c) of the said zone.

Geoelectrical sequence e4

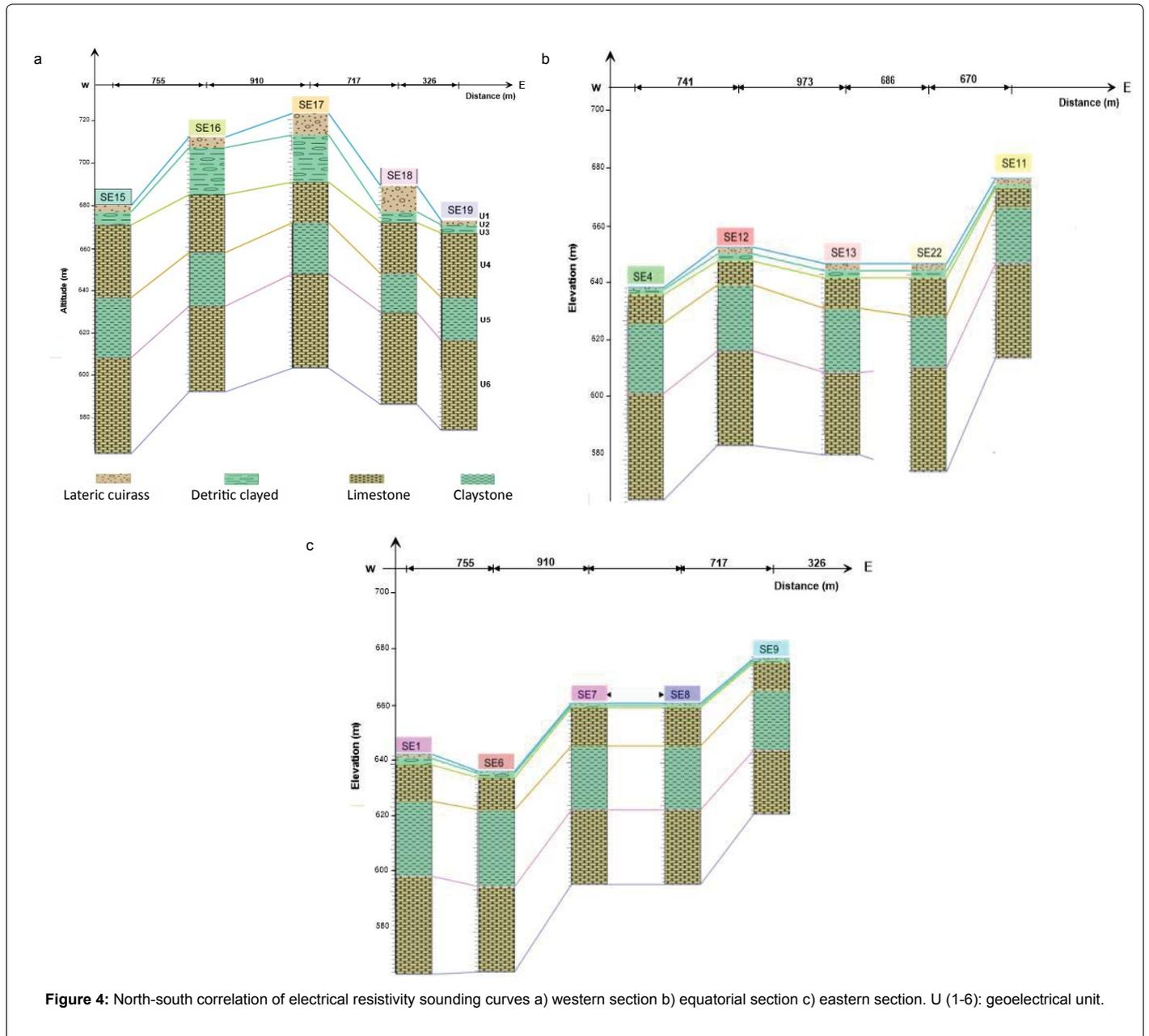
As of e4, it is a very thick sequence in all the sounding points and appears as a resistive level with resistivity between 1056 to 2544 Ω m. Its thickness generally increases from the northern towards the southern part of the study area (Figures 5a-5c).

Geoelectrical sequence e5

This sequence is visible at the end of sounding profiles and appears as a deep semi-conductive terrain with an average resistivity of 1209 Ω m at the 14 sounding point (Figure 5b).

Resistivity Curves to Borehole Correlation

Resistivity records over cores boreholes points as been performed (Figure 5a). These records permitted to correlate sedimentary units and geoelectrical sequences. The average resistivity and thicknesses of the different layers are summarized is given on Table 2.



Regarding e2 and e4 mineral ore bearing layers, the results of tridimensional modeling (Figure 6) indicate that their reserve can be estimate at 15343 m³ and 67989 m³ respectively.

Discussion and Conclusions

The results obtained show that the thickness of the ore bearing layers is almost constant (Figures 4 and 5). However, their variable geometry can either be due to post-deposition deformation or the original structure of the Dja Precambrian basin (Figure 5a). On the basis of geo-electrical parameters (Table 2), the Dja carbonate series is made up of seven petro physical units (U1, U2, U3, U4, U5, U6 and U7). The resistivity values associated carbonate ore bearing unit (Table

3) seems to be very continuous throughout the study area. These results are in good agreement with geo-electrical studies carried out in similar environments [23,24]. They also translate the relative homogeneity of the Dja carbonate ore bearing unit. Furthermore, the high resistivity values obtained from U3 at the sounding point 6 could have been associated to the very resistive nature of the subsurface capping layer (Figure 4c). While the low values observed at the sounding point 14 could be due to fluid circulation associated by N 55°E faulting. This observation was already made known by previous studies in the same study area by Ekoman [6]. In order to improve the results present on this paper, one of the solutions can be the densification of data grid acquisition or the use of 2D a multi-electrode resistivity acquisition.

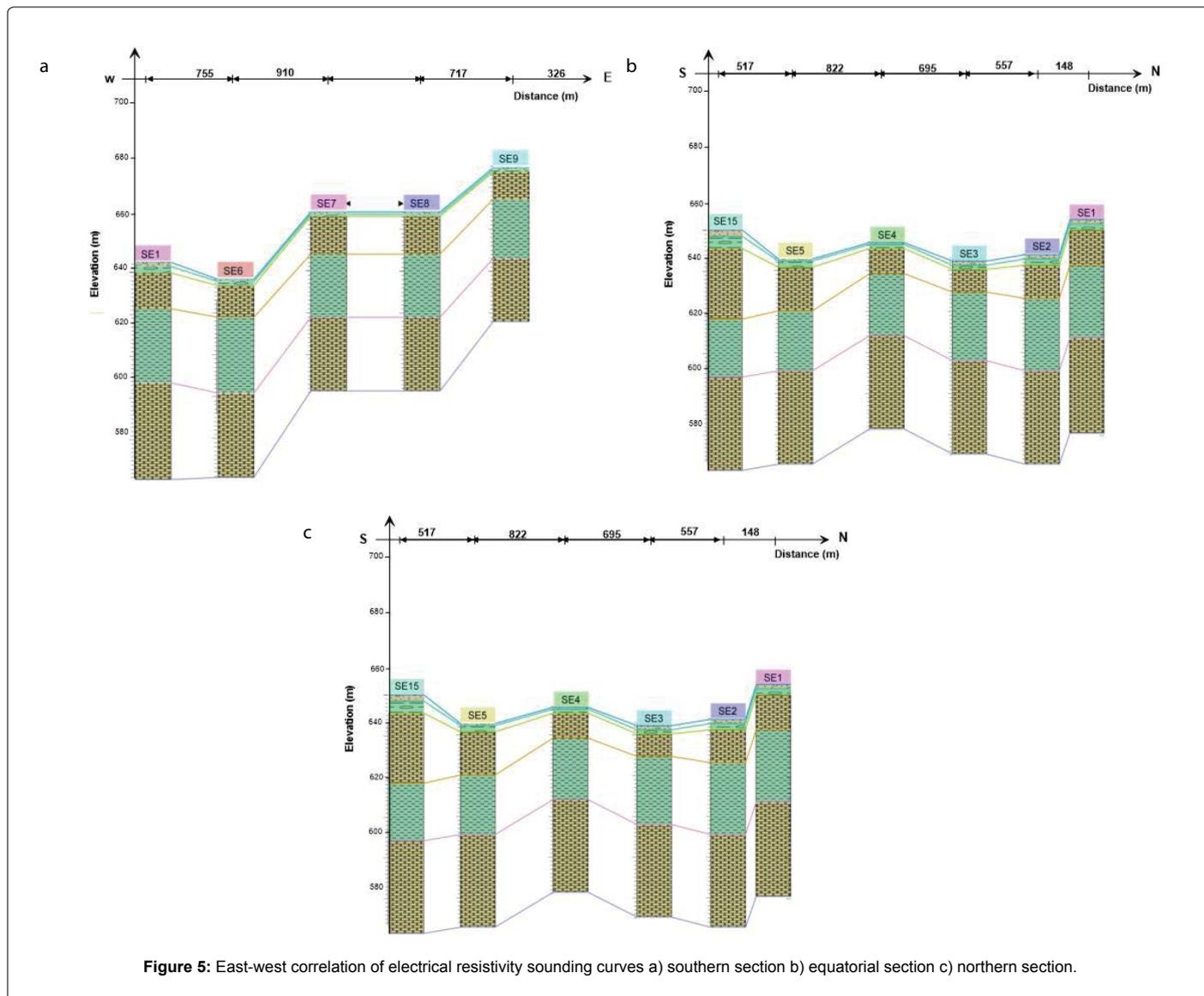


Figure 5: East-west correlation of electrical resistivity sounding curves a) southern section b) equatorial section c) northern section.

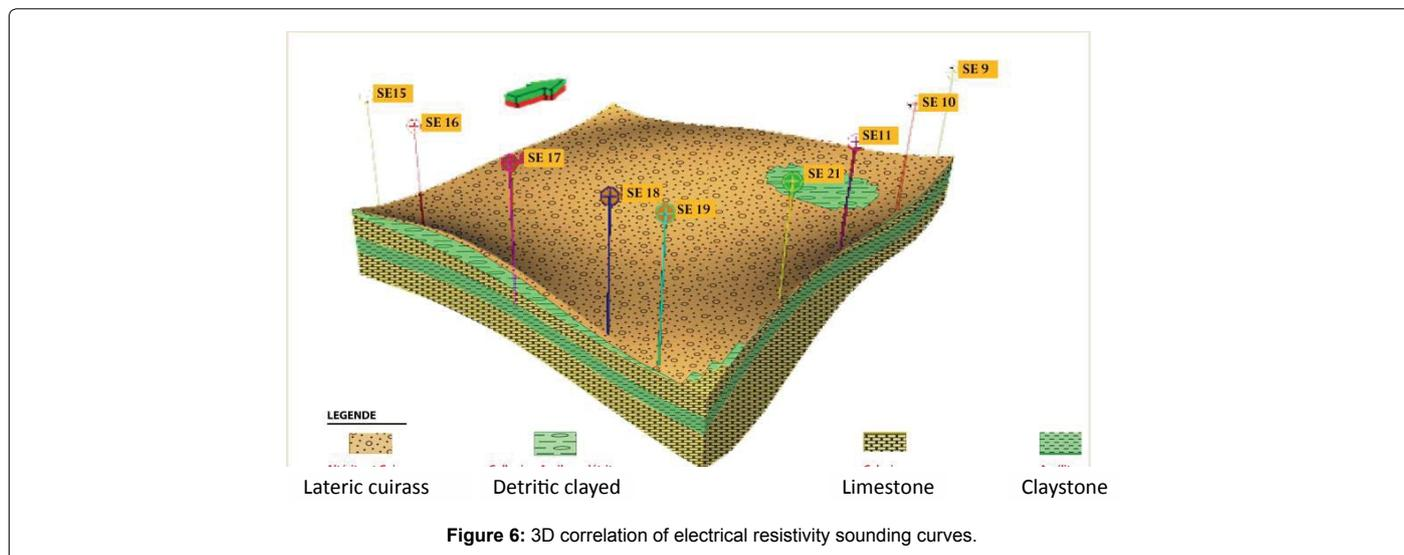


Figure 6: 3D correlation of electrical resistivity sounding curves.

Electrosequence	e1		e2	e3		e4	e5
Unit	U1	U2	U3	U4	U5	U6	U7
Resistivity (Ω m)	826-1068	5011-13545	1110-2377	181-440	225-746	1056-2544	1209
Thickness (m)	01-Dec	May-22	Nov-35	15-20	25-35	25-45	16-20
Lithology	Lateritic Cuirass	Clayey Colluvion	Massif Limestone	claystone	Shale	Massif limestone	Pelites

Table 2: Geoelectrical sequences and boreholes correlation.

e1	lateritic cuirass and detritic clayey deposits
e2	massif limestone of the Atog-Adjap unit
e3	claystone and shale
e4	massif limestone of the Metou unit
e5	alternation of pelite with a more or less carbonaceous deposits

Table 3: Recapitulation of the mapping ore bearing layers.

References

- Gazel J, Guiraudie C (1955) Mission of the descent of Dja-Missions Geological 1 and 2: Unpublished reports. Cameroon.
- Vanhoutte M, Salley P (1986) Mintom limestone reconstruction-mining research project, Southeast Cameroon. United Nations Development Program.
- United Nations Development Program (UNDP) (1987) Mining research in South East Cameroon.
- United Nations Development Program (UNDP) (1989) Review of the Mintom limestone geological survey and evaluation.
- Vicat JP (1998) Review of the knowledge gained on the series of Dja (Cameroon), Nola (Central African Republic) and Sembe-Ouessou (Congo). *Geosci in Cameroon*. 1: 369-383.
- Ekomane E (2010) Sedimentological and paleoenvironmental studies of the carbonate and pelitic rocks of the Mintom Formation (SE Cameroun).
- Caron V, Ekomane E, Mahieux G, Moussango P, Ndjeng E (2010) The mintom formation (new): Sedimentology and geochemistry of a neoproterozoic, paralic succession in south-east Cameroon. *J African Earth Sci* 57: 367-385.
- Caron V, Mahieux G, Ekomane E, Moussango P, Babinski M (2011) One, two or no record of late neoproterozoic glaciation in South-East Cameroon?. *J African Earth Sci* 59: 111-124.
- Gazel J, Hourcq V, Nichelès M (1956) Geological map of Cameroon.
- Vicat JP, Moloto-A-Kenguemba G, Pouclet A (2001) The granitoids of the proterozoic cover of the northern border of the Congo craton (south-eastern Cameroon and south-west of the Central African Republic), indicative of pre-Panafrican post-Kibarian magmatic activity. *Earth Planet Sci* 332: 235-242.
- Nzenti JP, Barbey P, Macaudière J, Soba D (1988) Origin and evolution of the late Precambrian high-grade Yaounde gneisses (Cameroon). *Precambrian Res* 38: 91-109.
- Censier C (1989) Sedimentary dynamics of a Mesozoic diamondiferous fluvial system. The formation of Carnot (Central African Republic).
- Telford WM, Geldaart LP, Sheriff RE (1990) *Applied Geophysics*. 2nd edn, Cambridge Univ Press.
- Albouy Y, Pion JC, Wackerman JM (1970) Application of electrical prospecting to the study of alteration levels. *Cah Orstom Ser Geol* 2: 161-170.
- Robain H, Descloitres M, Ritz M, Yene Atangana JQ (1996) A multiscale electrical survey of lateritic soil system in the rainforest of Cameroon. *J Appl Geophys* 34: 237-253.
- Ritz M, Robain H, Pervago E, Albouy Y, Camerlynch C (1999) Improvement to resistivity pseudo section modelling by removal of near surface inhomogeneity effect. *Geophys Prospect* 41: 85-101.
- Beauvais A, Ritz MM, Parisot JC, Dukhan M, Bantsimba C (1999) Analysis of poorly stratified lateritic terrains overlying a granitic bedrock in west Africa, using 2D electrical resistivity tomography. *Earth Planet Sci Lett* 173: 413-424.
- Keller GV, Frischknecht FC (1966) *Electrical methods in geophysical prospecting*. Pergamon Press, Oxford, pp: 519.
- Loke MH (1999) *Electrical imaging surveys for environmental and engineering studies. A practical guide to 2-D and 3-D surveys*, Penang, Malaysia.
- Storz H, Storz W, Jacobs F (2000) Electrical resistivity tomography to investigate geological structures of the earth's upper crust. *Geophys Prospect* 48: 455-471.
- Dahlin T, Zhou B (2004) A numerical comparison of 2D resistivity imaging with ten electrode arrays. *Geophy Prospec* 52: 379-398.
- Loke MH (1995) *Res2Dmod ver 2.20a 2D Resistivity forward modelling*. Malaysia.
- Revil A, Cathles LM, Losh S, Nunn JA (1998) Electrical conductivity in shaly sands with geophysical applications. *J Geophy Res* 103: 23925-23936.
- Revil A (2007) Final report on the mission of Tournemire. Large-scale electrical resistivity test at a test site.